Chemical and Biological Technologies in Agriculture

RESEARCH

Open Access

Antioxidant cellulose nanofibers/lignin-based aerogels: a potential material for biomedical applications

Laura M. Sanchez[1,2], Abigail K. Hopkins[3], Eduardo Espinosa[1*], Eneko Larrañeta[3], Dessislava Malinova[4], Adam Nathan McShane[4], Juan Domínguez-Robles[3,5*] and Alejandro Rodríguez[1]

Abstract

Background Lignin is a naturally occurring and aromatic biopolymer with well-known antimicrobial and antioxidant properties. Thus, in this work, the use of cellulose nanofibers (CNF) and lignin to produce ultra-light aerogels for biomedical applications was studied. Aerogels containing varying amounts of lignin (0–30 wt%) and different concentrations of the crosslinking agent Fe^{3+} (25–100 mM) were developed.

Results The different bioaerogels were fully characterized and their physical, mechanical and bioactive properties analyzed. It was observed that the bioaerogels soluble fraction tends to decrease as the lignin content increases for the different Fe^{3+} concentrations, due to lignin–CNF interactions through hydrogen bonds. The bioaerogels containing lignin showed remarkable radical scavenging activity as the DPPH concentration decreased with time. This confirms the benefits of including lignin in bioaerogels to impart antioxidant properties. To study the suitability of the produced bioaerogels for controlled drug release, the release of tetracycline (TC) was studied. All of the bioaerogels released TC in a sustained manner for 6 h and presented similar profiles. However, the bioaerogels containing higher concentrations of crosslinker showed a higher release of TC. The TC loading conferred clear antimicrobial activity against *S. aureus* as expected, unlike the insignificant antimicrobial activity of the bioaerogels without TC. The biocompatibility of the samples was demonstrated for all materials produced (with and without TC loading) by the Kruskal–Wallis test with multiple comparisons. After observation of cell morphology, no significant differences were evident suggesting that the CNF–lignin bioaerogels present optimal biocompatibility for use in the biomedical and pharmaceutical industry.

Conclusions The CNF–lignin bioaerogels presented in this work highlights their promising application as biomedical applications, such as wound dressings due to their biocompatibility, antimicrobial and antioxidant properties, as well as their swelling and solubility properties.

Keywords Lignocellulosic materials, Cellulose nanofibers, Lignin, Bioaerogels, Antioxidant properties, Antimicrobial dressings, Biocompatibility

*Correspondence:
Eduardo Espinosa
eduardo.espinosa@uco.es
Juan Domínguez-Robles
jdominguez6@us.es
Full list of author information is available at the end of the article

Springer Open

© The Author(s) 2023. **Open Access** This article is licensed under a Creative Commons Attribution 4.0 International License, which permits use, sharing, adaptation, distribution and reproduction in any medium or format, as long as you give appropriate credit to the original author(s) and the source, provide a link to the Creative Commons licence, and indicate if changes were made. The images or other third party material in this article are included in the article's Creative Commons licence, unless indicated otherwise in a credit line to the material. If material is not included in the article's Creative Commons licence and your intended use is not permitted by statutory regulation or exceeds the permitted use, you will need to obtain permission directly from the copyright holder. To view a copy of this licence, visit http://creativecommons.org/licenses/by/4.0/. The Creative Commons Public Domain Dedication waiver (http://creativecommons.org/publicdomain/zero/1.0/) applies to the data made available in this article, unless otherwise stated in a credit line to the data.

Graphical Abstract

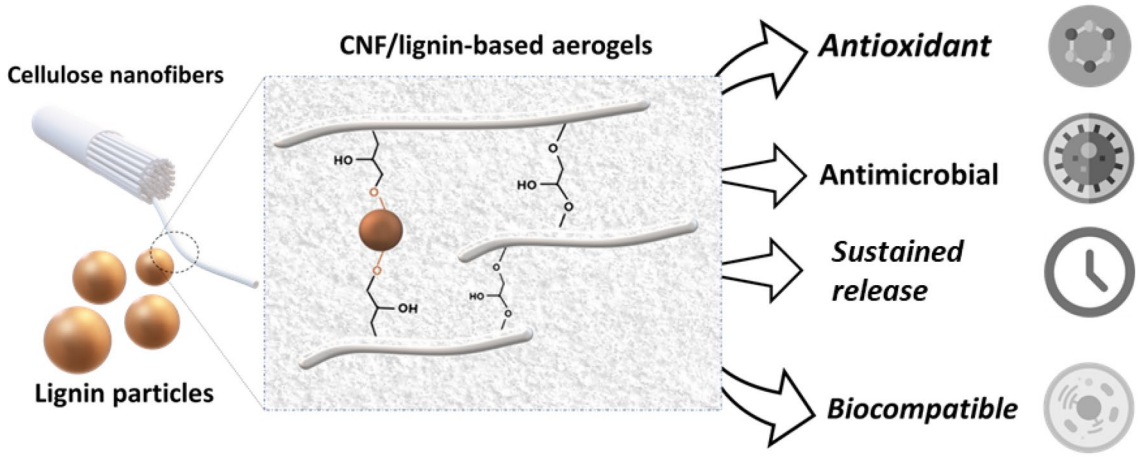

Introduction

Aerogels are porous solid materials that exhibit unique properties making them suitable for application in various fields. Their properties include low bulk density (< 0.5 g cm^{-3}), high and interconnected porosity (> 98%, mainly in the mesoporous range), large available specific surface area (> 150 m^2/g), as well as tunable surface chemistry [1]. In recent years, particular attention has been paid to the potential use of aerogels in biomedical applications, including tissue engineering, wound healing, drug delivery, implantable devices, sensing and diagnostics [2, 3]. However, for the use of aerogels in the development and manufacture of biomedical applications, these materials must demonstrate high biocompatibility, bioactivity, and good biodegradability, in addition to possessing adequate physicochemical properties.

Depending on the nature of the precursors, aerogels are usually divided into three main categories: inorganic, organic and hybrid aerogels [4]. Inorganic aerogels are mostly based on metals, oxides and silica, whereas organic aerogels are based on polymers (polystyrenes, polyurethanes, poly alcohols, polyacrylates). In the particular case of employing bio-derived polymers (polysaccharides, proteins, pectins, etc.) the materials are known as bioaerogels [5]. Bioaerogels possess cytocompatibility, biocompatibility and biodegradability functionalities, making them significantly more suited to applications in the biomedical sector than inorganic aerogels [6]. The biopolymers that constitute the lignocellulosic matrix are outstanding bioaerogel precursors since their processing preserves their bioactivity, biocompatibility and biodegradability, thus facilitating their application in the biomedical sector. Lignocellulosic materials are abundant, renewable and, for the most part, inexpensive resources and materials that are mainly derived from plant biomass, including agricultural waste [7]. The structural components of plant biomass are cellulose, hemicellulose and lignin, as well as other types of biopolymers such as proteins, peptides, etc.

Cellulose is the most abundant polysaccharide in nature, whereby it has been used as a replacement material for many oil-based products. In particular, it has attracted increasing interest in the biomedical sector due to its biocompatibility, thermal stability, renewability, biodegradability and harmlessness [8]. Two main processes are used to obtain cellulose aerogels: derivatization of cellulose followed by regeneration or by direct dissolution followed by coagulation or precipitation; in both cases forming crystalline forms (allomorphs) of cellulose II [9]. Another way to prepare cellulose aerogels without the need for dissolution processes (cellulose I) is the use of cellulose nanostructures (nanocellulose) as a precursor [10]. Nanocellulose are cellulose structures that have a dimension of 1–100 nm and can be isolated from natural cellulose fibers. One of the most common types of nanocellulose used in the production of cellulose-based aerogels are cellulose nanofibers (CNF). CNFs are isolated from natural fibers by delamination, i.e., by a strong mechanical treatment, and are 10–20 nm in diameter and several microns in length [11]. Owing to their nano-sized diameter and high specific surface area, low concentrations of solid matter are required for the formation of CNF gels (0.5–2%). Considering inherent properties and the nature of nanocellulose, CNF-based aerogels possess several desirable characteristics, including a high specific surface area, mechanical strength, surface activity,

porosity, and hydrophilicity. Unlike other applications, parameters such as biocompatibility and non-cytotoxicity are crucial for the development of biomedical applications using CNF-based aerogels. CNF with a high surface charge, such as those obtained through TEMPO-mediated oxidation (TO-CNF), have been found to be non-cytotoxic and devoid of irritation potential. Additionally, these CNF exhibit a promising antibacterial effect and can inhibit bacterial swimming properties [12]. These properties, combined with their ability to incorporate different materials (such as co-polymers, nanoparticles, etc.) during formulation, make them suitable for various purposes including drug delivery, scaffold fabrication, biosensors, diagnostics, antimicrobial dressings, medical implants, and vascular grafts [10, 13, 14].

Lignin is the most abundant naturally occurring aromatic macromolecule in nature. It is a natural polyphenolic polymer consisting of three main types of phenylpropane structural units: syringyl propane, guaiacol propane and p-hydroxyphenylpropane units [15, 16]. It also contains branched active functional groups, such as phenolic, hydroxyl, carboxylic carbonyl and methoxyl groups [17]. Lignin's natural origin, much like cellulose, ensures its high abundance, biocompatibility and biodegradability. Thus, presenting itself as an alternative to many synthetic polymers obtained from fossil fuels, for a wide range of applications [18–20]. In addition to the aforementioned advantages, lignin also exhibits antimicrobial and antioxidant properties [21]. These actions occur due to the effects of its phenolic structure on the bacterial envelope causing lysis, as well as its ability to act as hydrogen donor antioxidants [22]. All these characteristics make lignin a material with great potential for use in products with biomedical applications such as wound dressing materials [21, 23], drug delivery systems [24, 25], tissue engineering [26] and pharmaceutical excipients [17, 27]. The promising use of lignin in the production of aerogels is however associated with certain limitations due to its inability to self-crosslink. Therefore, it is mostly used as an additive mixed with other components such as formaldehyde, alginate, chitosan and poly(ethylene glycol) [25, 28–30].

The joint application of CNF and lignin to produce aerogels for biomedical applications is promising due to the desirable properties that these biomaterials exhibit. It has been shown that CNF–lignin hydrogen bonding interaction produces crosslinked 3D-lamellar porous aerogels with increased mechanical performance, density, adsorption and swelling capacity and specific surface area, as well as smaller pore size [31–33]. This combination of properties paves the way for its use in a multitude of applications in the biomedical and pharmaceutical sector. This study investigates the utilization of cellulose nanofibers (CNF) and lignin to create ultra-light aerogels for biomedical purposes. The physical, mechanical, and bioactive characteristics of various bioaerogels were analyzed by introducing varying quantities of lignin (0–30 wt%) and employing different concentrations of Fe3 + as a crosslinking agent (25–100 mM). Additionally, the release of tetracycline (TC) was evaluated to study the bioaerogels viability for controlled drug release. Furthermore, biocompatibility was established for all bioaerogels created (with or without TC loading) via the Kruskal–Wallis test with multiple comparisons.

Materials and methods

Materials

The reagents used in this work were: acetone (Sigma Aldrich); acetic acid (ACS reagent, ≥ 99.7%); hydrochloric acid (Sigma Aldrich, 37%); sodium chloride (Sigma Aldrich, > 99%); sodium hydroxide (Sigma Aldrich, > 99%); polydiallyldimethylammonium chloride (poly-DADMAC) (BTG, 0.01N); Pes-Na (BTG, 0.01N); TEMPO, 2,2,6,6-tetramethyl-piperidin-1-oxyle (Sigma Aldrich, 98%); sodium hypochlorite (Panreac, 10%); sodium bromide (Honeywell); Iron(III)chloride hexahydrate ($FeCl_3 \cdot 6H_2O$) (PanReac); hydrochloric acid (Panreac, 37%); phosphate buffer solution (PBS) at pH 7.4 was prepared using PBS tablets (Sigma Aldrich, Dorset, UK); Tetracycline hydrochloride (TC) (Sigma Aldrich, Dorset, UK); DPPH (2,2-diphenyl-1-picrylhydrazyl) (Sigma Aldrich, Dorset, UK). Staphylococcus aureus NCTC 10788 was incubated at 37 °C overnight in Mueller–Hinton (MH) broth before being used for the performance of the microbiological assay.

Wheat straw was kindly donated by an independent farmer from Córdoba, Spain. Wheat straw was subjected to an alkaline pulping process (100 °C, 150 min, 7% sodium hydroxide (over dry matter)), and a liquid/solid ratio of 10:1. Bleached pulp was obtained by a bleaching process with sodium chlorite (0.3 g per g of fiber) at 80 °C for 3 h. The chemical characterization of raw material and bleached pulp was reported in a previous work [34]. The chemical characterization for the raw material and bleached pulp was 39.7% and 68.2% α-cellulose (T-9m54), 17.7% and 1.9% lignin (T-203os61), 30.6% and 23.3% hemicelluloses (T-222), 7.7% and 2.9% ashes (T-211) and 5.2% and 0.7% alcohol extractables (T-204), respectively.

The lignin used was a softwood kraft lignin (BioPiva 100) acquired from UPM (Helsinki, Finland). To remove the moisture content of the lignin, it was placed in a forced-air circulated heating oven at 70 °C for 48 h. The characteristics of lignin have been described extensively by the manufacturer and by the authors in previous works [17]. The Klason lignin content according to TAPPI T 222 om-02 is about 92% of dry matter and the

acid-soluble lignin content according to TAPPI UM 250 is about 4% of dry matter. The sum of both components is commonly considered the value of the total lignin content in the sample (96%). The total amount of carbohydrates according to SCAN-CM 71:09 represents about 2% of the dry matter. The ash content by calcination at 700 °C represents about 1% of the dry matter. The molecular weight of lignin is between 5000 and 6000 Da.

Nanocellulose preparation and characterization

Cellulose nanofibers (TO-CNF) were isolated from bleached wheat straw pulp by TEMPO-mediated oxidation pretreatment. TEMPO-mediated oxidation at 5 mmol/g of cellulose was carried out adding the appropriate amount of 10% NaClO solution as oxidizing agent with continuous stirring at room temperature. A 0.5 M NaOH solution was used to maintain the pH reaction at 10 until no pH decrease was observed (around 2 h). The reaction was stopped by adding 10 mL of ethanol ant the fibers were washed with distilled water until neutral pH. This pretreatment has been proven in previous studies to be the most effective for the production of cellulose nanofibers of nanometric size and high surface charge, favoring their aqueous stability [35, 36]. After oxidation, a 1 wt% suspension of pretreated fiber was prepared and subjected to a high-pressure homogenization treatment in a PANDA 2000 (Gea Niro Soavi, Italy). The nanofibrillation treatment sequence followed was: 4 passes at 300 bar, 3 passes at 600 bar and 3 passes at 900 bar. The TO-CNF obtained were further characterized in accordance to several procedures previously reported by the authors [35–37].

Bioaerogels preparation

The bioaerogel samples were crosslinked through the hydrogelation methodology using a trivalent cation [38]. Different quantities of lignin (0, 15 and 30 wt% regarding the TO-CNF mass) were added to a TO-CNF aqueous suspension (0.7 wt%), and each mixture was stirred in a paddle mixer for 2 h. The homogenized dispersions (5 g) were then poured into Petri dishes, and 5 mL of Fe^{+3} solution (25, 50 and 100 mM) was added dropwise carefully along the container's walls. Each Petri dish was then maintained without stirring for 2 h and the resulting hydrogels were soaked and rinsed with a pH 3 HCl solution twice, and then with deionized water three times. Finally, the samples were lyophilized at − 83 °C at a vacuum pressure of 0.5 mBar for 48 h to obtain the nine desired bioaerogel samples. The preparation procedure is illustrated in Fig. 1. The bioaerogels samples were then abbreviated and named according to the amount lignin (0L, 15L and 30L) and the concentration of the Fe^{+3} solution (25Fe, 50Fe and 100Fe). For instance, the sample 30L-100Fe contained 30 wt% regarding the TO-CNF mass and 5 mL of a 100-mM Fe^{+3} solution.

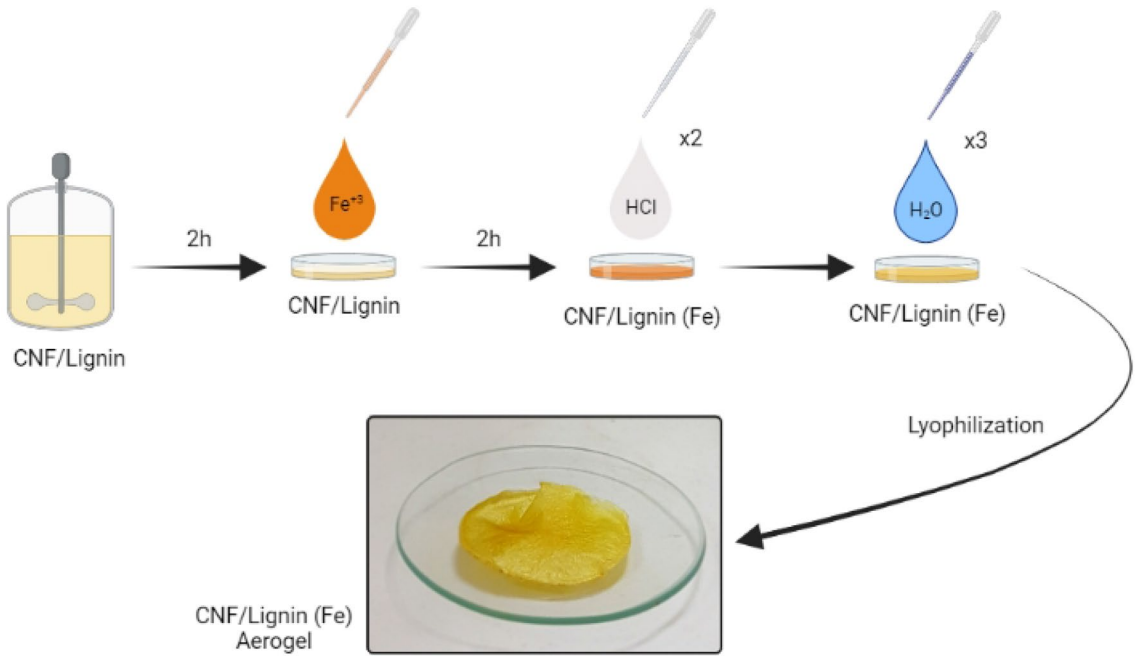

Fig. 1 CNF/lignin (Fe) bioaerogels preparation procedure

Bioaerogels characterization

The different bioaerogels were characterized. Through Fourier transform infrared spectroscopy analysis (FTIR) the possible chemical interactions between the TO-CNF, lignin and Fe^{3+} were explored. The FTIR spectra of the prepared materials were collected on an FTIR-ATR Perkin-Elmer Spectrum Two, in the range of 4000–500 cm^{-1} (employing a resolution of 4 cm^{-1} and 40 scans for each sample).

The swelling degree (SD %) properties of each sample at t time were determined in distilled water at 25 °C. The obtained data were processed using the following equation (Eq. 1):

$$SD(\%) = \frac{W_t - W_i}{W_i} \cdot 100, \quad (1)$$

where W_i is the weight of the bioaerogel before its immersion, and W_t corresponds to the weight of each sample at t time. Measurements were run in triplicate. Additionally, in order to determine the soluble fraction characteristics of the materials, a fixed mass of each bioaerogel was immersed in distilled water at 25 °C for 4 days. Then, each sample was removed from the aqueous medium and further dried until obtaining a constant weight. The soluble fraction (SF %) was calculated as follows (Eq. 2):

$$SF(\%) = \frac{W_i - W_f}{W_i} \cdot 100, \quad (2)$$

where W_i and W_f correspond to the weights of the dried bioaerogels before and after immersion, respectively. Measurements were run in triplicate.

Tetracycline release

All the bioaerogels were loaded with TC by placing a disc (8 mm diameter) of the respective bioaerogel into a glass vial containing 2 mL of a TC-deionized water solution (4 mg/mL). The vials were stored in the dark at room temperature for 24 h, to limit any degradation of the TC due to its photosensitivity. Then, discs were removed from the TC solution dried in the dark at room temperature for a duration of ≥ 48 h. The release kinetics of the TC-loaded bioaerogel discs was assessed by placing them into glass vials containing 5 mL PBS, to enable sink conditions. The vials were then incubated at 40 rpm and 37 °C. At defined intervals, 0.5 mL of solution was removed from each vial and the concentration of TC was assessed using a UV–Vis plate reader (PowerWave XS Microplate Spectrophotometer, Bio-Tek, Winooski, USA) at a wavelength of 363 nm, with $n = 4$ replicates for each condition. After each reading the medium was replaced with an equivalent volume of PBS. However, after the reading was taken at 24 h, the entire medium was removed and replaced with fresh PBS.

Antioxidant properties

A DPPH (2,2-diphenyl-1-picrylhydrazyl) radical was employed to measure the antioxidant activity of the different bioaerogel samples based on the radical scavenging property of the lignin [39, 40]. For this purpose, 5 mL of a DPPH solution dissolved in methanol (50 mg/L) was added to each vial containing a bioaerogel disc (8 mm diameter). A control sample of 50 mg/L of DPPH in methanol was also measured. The glass vials were then stored in the dark at room temperature. At defined time intervals, 300 µL of each sample was collected and the vials were immediately replenished with an equivalent volume of methanol. The absorbance of the different samples was analyzed using a UV–Vis plate reader (PowerWave XS Microplate Spectrophotometer, Bio-Tek, Winooski, VT, USA) at 517 nm, with n = 4 replicates for each condition. The residual DPPH content in the solution was calculated using Eq. 3:

$$\textit{Residual DPPH content}\ (\%) = 100 - 100\left(\frac{A_0 - A_1}{A_0}\right), \quad (3)$$

where A_0 is the absorbance of the control sample and A_1 is the absorbance in the presence of the sample at any time. Decreased absorbance of the reaction indicates a stronger DPPH radical scavenging activity.

Microbiology assay

Bioaerogel discs (8 mm diameter) containing either no TC or loaded with TC solution (4 mg/mL), as previously described, were tested for inhibitory effects on bacterial cultures of *Staphylococcus aureus* NCTC 10788. For this purpose, Mueller–Hinton (MH) broth was inoculated with *S. aureus* and then incubated overnight at 37 °C. 50 µL of this culture was added to 5 mL of soft MH agar and vortexed to ensure even distribution of the bacteria, the mixture was then poured on top of MH agar plates [41]. Bioaerogel discs were then placed on top of the agar and incubated at 37 °C for 24 h. The inhibition zone caused for *S. aureus* was measured in mm. Furthermore, inoculated plates with *S. aureus* alone were also incubated as positive control. The results were expressed as mean ± standard deviation, with $n = 4$ replicates for each condition.

Cytocompatibility test

HEK293T (human embryonic kidney, ATCC) cells were seeded in DMEM (Dulbecco's modified Eagle medium), supplemented with 10% fetal calf serum and

non-essential amino acids, in a 24-well plate at 20,000 cells per well and allowed to adhere overnight at 37 °C. An equal volume of culture media pre-incubated with compound was added to each well. Three independent samples of each compound were used. On day 3 post-treatment, cells were imaged on an Olympus widefield microscope using 20× objective. One representative image is shown from each condition. Cells adhered in all conditions and cell growth was comparable. On day 3 post-culture, cell viability was measured using an MTT assay (3-(4,5-dimethylthiazol-2-yl)-2,5-diphenyltetrazolium, Merck).

Statistical analysis

All quantitative data were expressed as mean ± standard deviation. Statistical analysis was performed using a one-way analysis of variance (ANOVA), followed by a multiple comparison test (Tukey's test) to assess whether there were significant differences between the means of the data sets as appropriate. In all cases, p-value < 0.05 indicated a statistically significant difference between tested groups.

Results and discussion

Bioaerogel preparation and characterization

By varying both the lignin and the Fe^{3+} concentrations, it was possible to successfully obtain nine different bioaerogel samples (Additional file 1: Figure S1). As expected, the different materials did not present any new covalent chemical interactions (Additional file 1: Figure S2). The bioaerogels swelling properties (Fig. 2) were tested considering both the Fe^{3+} and lignin contents. It was expected that the higher the lignin content, the lower the swelling degree capacities due to lignins intrinsic hydrophobicity. The results did not reflect the predicted relationship between lignin and the swelling degree, most likely because the lignin particles were enclosed in the CNF, acting as crosslinking dots. The different Fe^{+3} concentrations did appear to have some effect on the bioaerogels swelling properties with low lignin contents, however this effect was not easy to spot. The degree of swelling increased as the content of Fe^{+3} also increased, ranging from 25 to 50 mM. However, higher quantities of cations resulted in the opposite trend. This phenomenon may be explained in terms of the formation of Fe^{+3} agglomerates, as it was previously observed in other physically crosslinked gel materials [42]. Additionally, it is of key importance to keep in mind that this property is strongly dependent on several of the material's network characteristics, such as pore size and morphology, crystallinity degree and gel/soluble fraction [43, 44].

The soluble fraction of the different samples appeared to decrease as the lignin content increased for the three considered Fe^{3+} concentrations (Fig. 3). These results are in accordance with those expected, since lignin and CNF can successfully interact through hydrogen bonding. Thus, lignin acts as effective crosslinking dots in which CNF are encompassing lignin particles [31, 33]. Furthermore, the presence or absence of lignin has a stronger effect on this property than the trivalent cation concentrations. The inclusion of Fe^{+3} only exerts certain undesired negative effect on the materials soluble fraction when considering the highest cation concentration. On the other hand, in the 30L bioaerogel materials the employment of different Fe^{3+} concentrations made little difference to the materials solubility. This can be related to the fact that the trivalent cation was added to the CNF/lignin mixture after 2 h time, during which these two components are able to establish a high number of

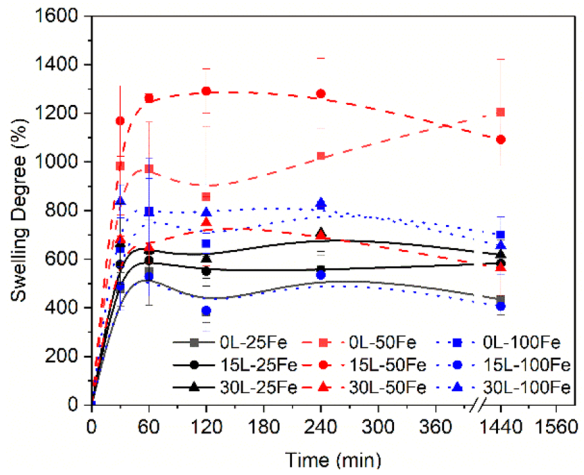

Fig. 2 Swelling degree properties of the bioaerogels

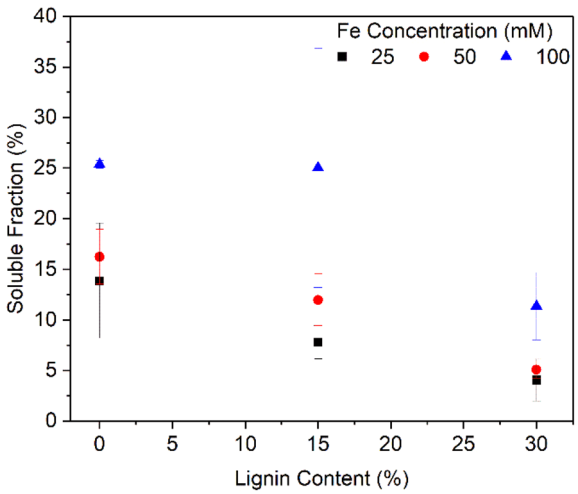

Fig. 3 Soluble fraction of the bioaerogels

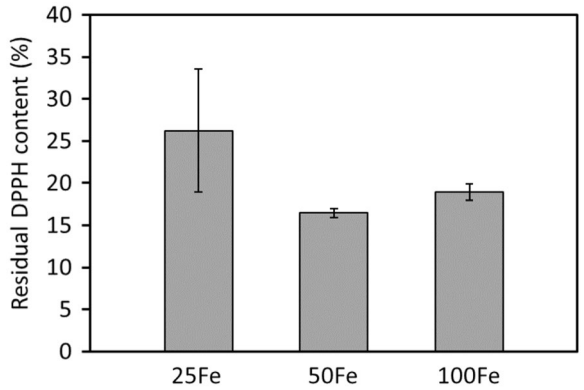

Fig. 4 Residual DPPH content for the lignin-based bioaerogels using an initial DPPH concentration of 50 mg/L at 360 min, with $n = 4$ replicates for each condition

hydrogen bonds, leading to small quantities of CNF capable of further interacting with the Fe^{3+} cations. From the obtained results, the three 30L bioaerogel materials were selected to be further tested.

Antioxidant properties of the bioaerogels

In order to assess the antioxidant properties of the lignin-based bioaerogels, a DPPH assay was performed (Fig. 4). All of the lignin-based bioaerogels showed remarkable radical scavenging activity as the DPPH concentration was decreased over time. Thus, these results indicate that the presence of lignin provided all the bioaerogels with antioxidant properties. The 50Fe and 100Fe bioaerogel samples were able to considerably reduce the DPPH concentration up to *ca*. 84% and 81% after 360 min, and no significant differences were found between these two samples ($p = 0.6998$). The 25Fe samples exhibited significantly lower antioxidant activity at the same time (74%) in comparison to 50Fe bioaerogel sample ($p < 0.05$), however, no significant differences were found between 25 and 50Fe bioaerogel samples ($p = 0.0897$). These results are similar to those found in different studies, where lignin was incorporated within thermoplastic matrices, such as poly(butylene succinate), polylactic acid (PLA) or poly(caprolactone) for achieving antioxidant composite materials [21, 39, 40]. Antioxidant materials, such as these bioaerogels, have the potential to be used for the development of biomedical devices. Materials exhibiting antioxidant properties are able to reduce the concentration of reactive oxygen species (ROS) and free radicals [45, 46]. The presence of high concentrations of ROS has been shown to interfere and possibly prevent the wound healing process [47, 48]. Thus, the bioaerogels developed in this study show promising antioxidant properties and therefore could be used as wound dressings to help accelerate the wound healing process.

Tetracycline release from bioaerogels

The release of TC from the bioaerogel discs was evaluated for 24 h. The bioaerogels were capable of providing a sustained TC release for 6 h (Fig. 5). Moreover, it can be seen that all the release profiles had similar shapes. However, bioaerogels containing higher amounts of iron (50Fe and 100Fe bioaerogel samples) showed a higher TC release compared to those containing the lowest amount of iron (25Fe bioaerogel samples). Statistical analysis revealed that there were significant differences between the 25Fe bioaerogel samples and the other 50Fe and 100Fe bioaerogel samples ($p < 0.05$). However, no significant differences were found between the 50Fe and 100Fe bioaerogel samples ($p > 0.05$). As previously proposed and reported, TC could bind either Fe^{2+} or Fe^{3+} [49, 50]. Therefore, it can be hypothesized that TC could be interacting with iron ions within the bioaerogel matrix. This interaction may result in a higher drug loading for those samples containing a higher amount of iron (50Fe and 100Fe bioaerogel samples) and thus this might explain the difference in drug release observed in this study.

The total amount of TC released after 6 h ranged from 115 to 152 µg. This range of released drug was similar to those found in other studies, where different antibiotic-loaded medical devices were manufactured and exhibited antimicrobial properties [51, 52]. Therefore, the TC-loaded bioaerogels demonstrated their potential for use as dressings for the treatment of wound infections that if left untreated can significantly delay and disrupt the healing process [53]. These outcomes are in line with those discussed in the previous section (antioxidant properties).

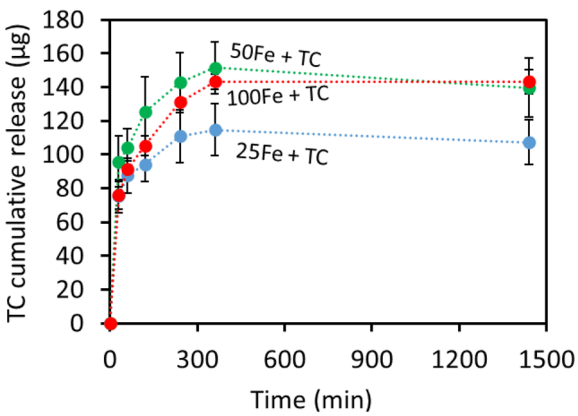

Fig. 5 In vitro TC release curves from TC-loaded bioaerogels in PBS at 37 °C expressed in µg as function of time, with $n = 4$ replicates for each condition

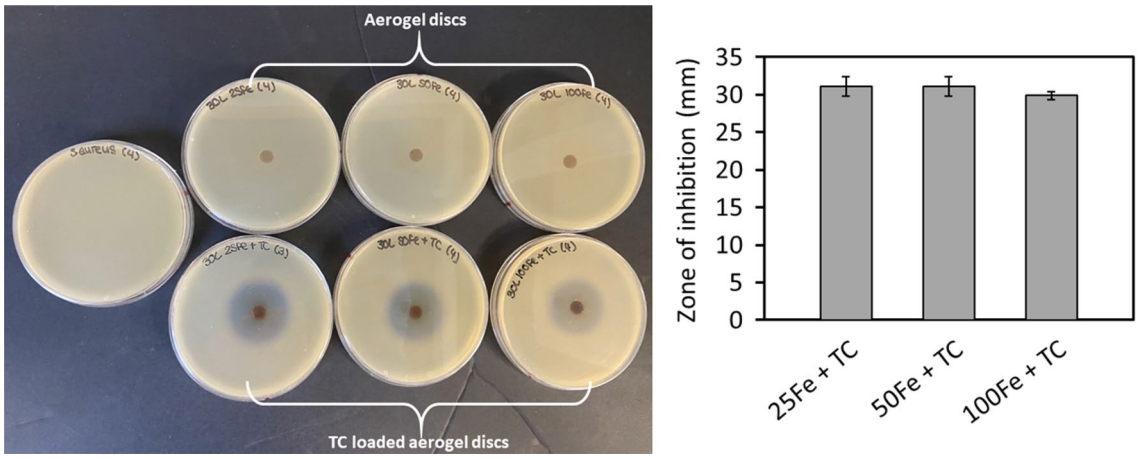

Fig. 6 A picture showing the zone of inhibition obtained for *S. aureus* in MH agar using bioaerogel discs containing either no TC or loaded with TC solution (4 mg/mL), with $n = 4$ replicates for each condition

Antimicrobial properties of bioaerogels

The antimicrobial activity of TC-loaded bioaerogel discs was tested using a bacterial culture of *S. aureus.* The results of the disk diffusion experiment are shown in Fig. 6. As expected, all the TC-loaded bioaerogel discs exhibited clear antimicrobial activity against *S. aureus* (Fig. 6). The diameter of the zone of inhibition in the *S. aureus* plates containing these TC-loaded bioaerogel discs ranged from 29.88 ± 0.48 mm to 31.13 ± 1.31 mm. However, no significant differences were found between the different bioaerogel formulations used for this purpose ($p > 0.05$). Moreover, the same bioaerogel formulations containing no TC were also tested on the same bacterial strain to evaluate if the bioaerogels themselves exhibited any antimicrobial properties (Fig. 6A). However, no zone of inhibition was observed in plates containing these control bioaerogel discs without TC. Although it has been reported that lignin has antimicrobial activity [22, 54, 55], the presence of lignin was not able to provide sufficient antimicrobial properties to the bioaerogels. The loading of drug molecules, such as TC, into the bioaerogels provided them with notable antimicrobial activity. Once again, the bioaerogels have potential to be used for biomedical applications and, more

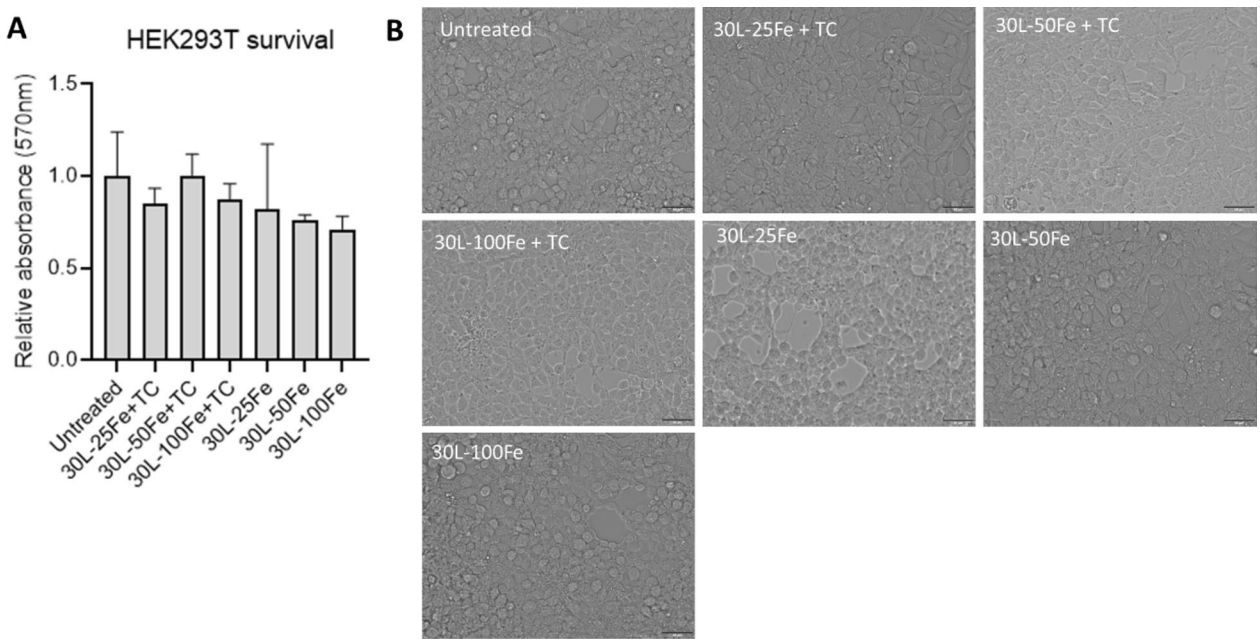

Fig. 7 In vitro cell cytocompatibility in HEK293T cells using an MTT assay (**A**). Cell morphology obtained post-treatment using a 20 × objective (**B**)

specifically, for the manufacture of wound dressings, since these materials could also help prevent infections.

In vitro cytocompatibility of the bioaerogels

In order to ascertain the cytocompatibility of the materials prepared in this work, HEK293T cells were used. This cell line has been used in the past to study the cytocompatibility of different types of biomaterials [56–58]. Figure 7 shows the MTT test results. The Kruskal–Wallis test with multiple comparisons results show there was no significant difference between the untreated control group and the other samples. Additionally, cell morphology was observed using a widefield microscope 3 days post-treatment with the bioaerogels. In all cases cell morphology was like that observed for the untreated cell group, indicating cell morphology remained unaffected upon treatment with the aerogels. These results suggest that the materials prepared in this work are biocompatible.

These results are not surprising considering that the biocompatibility of the components present in the bioaerogels has been reported in the past. The biocompatibility of TEMPO-oxidized nanocellulose and Fe^{3+} has been extensively evaluated suggesting that this material presents excellent cytocompatibility and hemocompatibility [59, 60]. The biocompatibility of lignin is not as clearly defined, however lignin-based biomaterials have been proven to be cytocompatible or to show low cytotoxicity [61–63]. Finally, TC has been reported to be biocompatible in several animal studies [64, 65].

Conclusions

Studies on the properties of lignin have outlined its potent antioxidant and antimicrobial activity, and its promising application within the biomedical sector; as well as highlighting the limitations caused by its inability to self-crosslink. In this study bioaerogels containing CNF, lignin and the crosslinker Fe^{3+} were developed and fully characterized to investigate the bioaerogels properties when different concentrations of lignin and Fe^{3+} were introduced.

Lignin exhibited strong radical scavenging activity that gave the bioaerogels potent antioxidant properties capable of reducing ROS concentrations and potentially accelerating wound healing. The bioaerogels swelling degree was unaffected by increasing lignin concentrations, suggesting inclusion of lignin in the CNF masks its intrinsic hydrophobicity. Comparatively, the bioaerogels solubility fraction was decreased by increasing lignin concentration as a result of the lignin–CNF interactions. Despite lignins previously characterized antimicrobial activity, these lignin bioaerogels exhibited no notable inhibition of *S. aureus*. However, upon loading the bioaerogels with TC, they exhibited potent antimicrobial activity and sustained TC release over 6 h. Inclusion of high Fe^{3+} concentrations appeared to promote the bioaerogels release of TC as well as its antioxidant activity, most likely through its crosslinking action. The bioaerogels also demonstrated optimal biocompatibility, highlighting their suitability for biomedical applications.

In conclusion, this study characterizes the antioxidant activity, biocompatibility, TC release, swelling and solubility properties of CNF bioaerogels containing lignin and Fe^{3+}, and highlights their promising application as wound dressings.

Supplementary Information

The online version contains supplementary material available at https://doi.org/10.1186/s40538-023-00438-z.

Additional file 1: Figure S1. Pictures of the aerogel samples. **Figure S2**. FTIR spectra of the aerogel samples: 0% Lignin a) 25Fe, b) 50Fe, c) 100Fe; 15% Lignin d) 25Fe, e) 50Fe, f) 100Fe; 30% Lignin g) 25Fe, h) 50Fe, i) 100Fe; j).

Acknowledgements

Authors acknowledge the financial support to the Ministerio de Ciencia e Innovación (MCINN) of Spain in the form of a national project, PID2020-117718RB-I00, as part of the national programme of R+D projects «Retos Investigación» y «Generación de Conocimiento», funded by MCIN/AEI/10.13039/501100011033. Juan Domínguez-Robles acknowledges financial support from the Ramón y Cajal grant RYC-2021-034357-I funded by MCIN/AEI/10.13039/501100011033 and by the "European Union NextGenerationEU/PRTR". Laura M. Sanchez acknowledges the financial support of CONICET, ANPCyT (PICT-2018-0711) and UNMdP, and she was benefited from conversations during her research stays supported by Fundación Carolina, Fundación Bunge y Born and Fulbright Argentina - Ministerio de Educación. BioRender.com was used to create Figures. The authors also thank the staff of Microscopy unit of the Central Research Support Service (SCAI) and to the staff of Instituto Químico para la Energía y el Medioambiente (IQUEMA) of the Universidad de Córdoba. This work was also financially supported by the Society for Applied Microbiology (*Sf*AM) through the funding of a summer student placement scholarship.

Author contributions

LMS: conceptualization, methodology, funding acquisition, investigation, formal analysis. AKH: methodology, investigation, formal analysis. ee: supervision, conceptualization, methodology, investigation, formal analysis. EL: supervision, conceptualization, funding acquisition, formal analysis. DM: supervision, conceptualization, formal analysis. ANMcS: methodology, investigation, formal analysis. JD-R: supervision, conceptualization, methodology, funding acquisition, investigation, formal analysis. AR: supervision, conceptualization, funding acquisition, formal analysis. All authors wrote the original draft and reviewed the manuscript.

Funding

Ramón y Cajal grant RYC-2021-034357-I funded by MCIN/AEI/10.13039/501100011033 and by the "European Union NextGenerationEU/PRTR". Ministerio de Ciencia e Innovación (MCINN) of Spain in the form of a national project, PID2020-117718RB-I00, as part of the national programme of R+D projects «Retos Investigación» y «Generación de Conocimiento», funded by MCIN/AEI/10.13039/501100011033. CONICET, ANPCyT (PICT-2018-0711), UNMdP, Fundación Carolina, Fundación Bunge y Born and Fulbright Argentina - Ministerio de Educación. Society for Applied Microbiology (*Sf*AM) through the funding of a summer student placement scholarship.

Declarations

Ethics approval and consent to participate
Not applicable.

Consent for publication
Not applicable.

Competing interests
The authors declare that they have no competing interests. The results/data/figures in this manuscript have not been published elsewhere, nor are they under consideration (from you or one of your Contributing Authors) by another publisher. All of the materials in this manuscript are owned by the authors and/or no permissions are required.

Author details
[1]Chemical Engineering Department, Faculty of Science, BioPrEn Group (RNM 940) Instituto Químico Para La Energía Y El Medioambiente (IQUEMA) Universidad de Córdoba, 14014 Córdoba, Spain. [2]Materiales Compuestos Termoplásticos (CoMP), Instituto de Investigaciones en Ciencia Y Tecnología de Materiales (INTEMA), CONICET - Universidad Nacional de Mar del Plata (UNMdP), Av. Colón 10850, 7600 Mar del Plata, Argentina. [3]School of Pharmacy, Queen's University Belfast, Belfast, UK. [4]Wellcome-Wolfson Institute for Experimental Medicine, Queen's University Belfast, Belfast, UK. [5]Department of Pharmacy and Pharmaceutical Technology, University of Seville, Seville, Spain.

Received: 18 May 2023 Accepted: 10 July 2023
Published online: 07 August 2023

References

1. Manzocco L, Mikkonen KS, García-González CA. Aerogels as porous structures for food applications: smart ingredients and novel packaging materials. Food Struct. 2021;28: 100188.
2. Ferreira-Gonçalves T, Constantin C, Neagu M, Reis CP, Sabri F, Simón-Vázquez R. Safety and efficacy assessment of aerogels for biomedical applications. Biomed Pharmacother. 2021;144: 112356.
3. Okutucu B. The medical applications of biobased aerogels: natural aerogels for medical usage. Med Devices Sens. 2021. https://doi.org/10.1002/mds3.10168.
4. Ferreira-Gonçalves T, Iglesias-Mejuto A, Linhares T, Coelho JMP, Vieira P, Faísca P, et al. Biological thermal performance of organic and inorganic aerogels as patches for photothermal therapy. Gels. 2022;8:1–18.
5. Moheman A, Bhawani SA, Tariq A. Aerogels for waterborne pollutants purification. Adv Aerogel Compos Environ Remediat. 2021. https://doi.org/10.1016/B978-0-12-820732-1.00007-2.
6. Shi W, Ching YC, Chuah CH. Preparation of aerogel beads and microspheres based on chitosan and cellulose for drug delivery: a review. Int J Biol Macromol. 2021;170:751–67.
7. Budtova T, Aguilera DA, Beluns S, Berglund L, Chartier C, Espinosa E, et al. Biorefinery approach for aerogels. Polym. 2020. https://doi.org/10.3390/polym12122779.
8. Moohan J, Stewart SA, Espinosa E, Rosal A, Rodríguez A, Larrañeta E, et al. Cellulose nanofibers and other biopolymers for biomedical applications. A review. Appl Sci. 2020. https://doi.org/10.3390/app10010065.
9. Budtova T. Cellulose II aerogels: a review. Cellulose. 2019;26:81–121.
10. Lavoine N, Bergström L. Nanocellulose-based foams and aerogels: processing, properties, and applications. J Mater Chem A. 2017;5:16105–17.
11. Espinosa E, Rol F, Bras J, Rodríguez A. Production of lignocellulose nanofibers from wheat straw by different fibrillation methods. Comparison of its viability in cardboard recycling process. J Clean Prod. 2019. https://doi.org/10.1016/j.jclepro.2019.118083.
12. Chinga-Carrasco G, Johansson J, Heggset EB, Leirset I, Björn C, Agrenius K, et al. Characterization and antibacterial properties of autoclaved carboxylated wood nanocellulose. Biomacromol. 2021;22:2779–89. https://doi.org/10.1021/acs.biomac.1c00137.
13. Abdul Khalil HPS, Adnan AS, Yahya EB, Olaiya NG, Safrida S, Hossain MS, et al. A review on plant cellulose nanofibre-based aerogels for biomedical applications. Polymers. 2020. https://doi.org/10.3390/polym12081759.
14. Chen Y, Zhang L, Yang Y, Pang B, Xu W, Duan G, et al. Recent progress on nanocellulose aerogels: preparation, modification, composite fabrication, applications. Adv Mater. 2021;33:2005569. https://doi.org/10.1002/adma.202005569.
15. Domínguez-Robles J, Tamminen T, Liitiä T, Peresin MS, Rodríguez A, Jääskeläinen A-S. Aqueous acetone fractionation of kraft, organosolv and soda lignins. Int J Biol Macromol. 2018. https://doi.org/10.1016/j.ijbiomac.2017.08.102.
16. Boerjan W, Ralph J, Baucher M. Lignin biosynthesis. Annu Rev Plant Biol. 2003;54:519–46. https://doi.org/10.1146/annurev.arplant.54.031902.134938.
17. Domínguez-Robles J, Stewart SASA, Rendl A, González Z, Donnelly RFRF, Larrañeta E. Lignin and cellulose blends as pharmaceutical excipient for tablet manufacturing via direct compression. Biomolecules. 2019. https://doi.org/10.3390/biom9090423.
18. Moreno A, Sipponen MH. Lignin-based smart materials: a roadmap to processing and synthesis for current and future applications. Mater Horizons. 2020;7:2237–57.
19. Domínguez-Robles J, Peresin MS, Tamminen T, Rodríguez A, Larrañeta E, Jääskeläinen A-S. Lignin-based hydrogels with "super-swelling" capacities for dye removal. Int J Biol Macromol. 2018. https://doi.org/10.1016/j.ijbiomac.2018.04.044.
20. Domínguez-Robles J, Espinosa E, Savy D, Rosal A, Rodríguez A. Biorefinery process combining Specel® process and selective lignin precipitation using mineral acids. BioResources. 2016. https://doi.org/10.15376/biores.11.3.7061-7077.
21. Domínguez-Robles J, Cuartas-Gómez E, Dynes S, Utomo E, Anjani QK, Detamornrat U, et al. Poly(caprolactone)/lignin-based 3D-printed dressings loaded with a novel combination of bioactive agents for wound-healing applications. Sustain Mater Technol. 2023;35:e00581.
22. Aadil KR, Mussatto SI, Jha H. Synthesis and characterization of silver nanoparticles loaded poly(vinyl alcohol)-lignin electrospun nanofibers and their antimicrobial activity. Int J Biol Macromol. 2018;120:763–7.
23. Zhang Y, Jiang M, Zhang Y, Cao Q, Wang X, Han Y, et al. Novel lignin–chitosan–PVA composite hydrogel for wound dressing. Mater Sci Eng C. 2019;104: 110002.
24. Zhou Y, Han Y, Li G, Yang S, Xiong F, Chu F. Preparation of targeted lignin-based hollow nanoparticles for the delivery of doxorubicin. Nanomaterials. 2019. https://doi.org/10.3390/nano9020188.
25. Larrañeta E, Imízcoz M, Toh JXJX, Irwin NJNJ, Ripolin A, Perminova A, et al. Synthesis and characterization of lignin hydrogels for potential applications as drug eluting antimicrobial coatings for medical materials. ACS Sustain Chem Eng. 2018;6:9037–46.
26. Saudi A, Amini S, Amirpour N, Kazemi M, Zargar Kharazi A, Salehi H, et al. Promoting neural cell proliferation and differentiation by incorporating lignin into electrospun poly(vinyl alcohol) and poly(glycerol sebacate) fibers. Mater Sci Eng C. 2019;104: 110005.
27. Pishnamazi M, Hafizi H, Shirazian S, Culebras M, Walker GM, Collins MN. Design of controlled release system for paracetamol based on modified lignin. Polymers. 2019. https://doi.org/10.3390/polym11061059.
28. Grishechko LI, Amaral-Labat G, Szczurek A, Fierro V, Kuznetsov BN, Celzard A. Lignin–phenol–formaldehyde aerogels and cryogels. Microporous Mesoporous Mater. 2013;168:19–29.
29. Ravishankar K, Venkatesan M, Desingh RP, Mahalingam A, Sadhasivam B, Subramaniyam R, et al. Biocompatible hydrogels of chitosan-alkali lignin for potential wound healing applications. Mater Sci Eng C. 2019;102:447–57.
30. Quraishi S, Martins M, Barros AA, Gurikov P, Raman SP, Smirnova I, et al. Novel non-cytotoxic alginate–lignin hybrid aerogels as scaffolds for tissue engineering. J Supercrit Fluids. 2015;105:1–8.
31. Xia J, Liu Z, Chen Y, Cao Y, Wang Z. Effect of lignin on the performance of biodegradable cellulose aerogels made from wheat straw pulp-LiCl/DMSO solution. Cellulose. 2020;27:879–94.
32. Berglund L, Forsberg F, Jonoobi M, Oksman K. Promoted hydrogel formation of lignin-containing arabinoxylan aerogel using cellulose nanofibers as a functional biomaterial. RSC Adv. 2018;8:38219–28.
33. Wang C, Xiong Y, Fan B, Yao Q, Wang H, Jin C, et al. Cellulose as an adhesion agent for the synthesis of lignin aerogel with strong mechanical

performance, Sound-absorption and thermal Insulation. Sci Rep. 2016;6:1–9.
34. Espinosa E, Rol F, Bras J, Rodríguez A. Use of multi-factorial analysis to determine the quality of cellulose nanofibers: effect of nanofibrillation treatment and residual lignin content. Cellulose. 2020. https://doi.org/10.1007/s10570-020-03136-3.
35. Espinosa E, Sánchez R, Otero R, Domínguez-robles J, Rodríguez A. A comparative study of the suitability of different cereal straws for lignocellulose nanofibers isolation. Int J Biol Macromol. 2017;103:990–9.
36. Espinosa E, Domínguez-Robles J, Sánchez R, Tarrés Q, Rodríguez A. The effect of pre-treatment on the production of lignocellulosic nanofibers and their application as a reinforcing agent in paper. Cellulose. 2017. https://doi.org/10.1007/s10570-017-1281-2.
37. Espinosa E, Bascón-Villegas I, Rosal A, Pérez-Rodríguez F, Chinga-Carrasco G, Rodríguez A. PVA/(ligno)nanocellulose biocomposite films. Effect of residual lignin content on structural, mechanical, barrier and antioxidant properties. Int J Biol Macromol. 2019;141:197–206.
38. Dong H, Snyder JF, Williams KS, Andzelm JW. Cation-induced hydrogels of cellulose nanofibrils with tunable moduli. Biomacromol. 2013;14:3338–45.
39. Domínguez-Robles J, Larrañeta E, Fong MLML, Martin NKNK, Irwin NJNJ, Mutjé P, et al. Lignin/poly(butylene succinate) composites with antioxidant and antibacterial properties for potential biomedical applications. Int J Biol Macromol. 2020;145:92–9.
40. Domínguez-Robles J, Martin NKNK, Fong MLML, Stewart SASASA, Irwin NJNJ, Rial-Hermida MIMI, et al. Antioxidant pla composites containing lignin for 3D printing applications: a potential material for healthcare applications. Pharmaceutics. 2019. https://doi.org/10.3390/pharmaceutics11040165.
41. Domínguez-Robles J, Utomo E, Cornelius VA, Anjani QK, Korelidou A, Gonzalez Z, et al. TPU-based antiplatelet cardiovascular prostheses prepared using fused deposition modelling. Mater Des. 2022;220:110837.
42. Sanchez LM, Shuttleworth PS, Waiman C, Zanini G, Alvarez VA, Ollier RP. Physically-crosslinked polyvinyl alcohol composite hydrogels containing clays, carbonaceous materials and magnetic nanoparticles as fillers. J Environ Chem Eng. 2020;8:103795.
43. Kokabi M, Sirousazar M, Hassan ZM. PVA-clay nanocomposite hydrogels for wound dressing. Eur Polym J. 2007;43:773–81.
44. Sanchez LM, Alvarez VA, Ollier RP. Acid-treated Bentonite as filler in the development of novel composite PVA hydrogels. J Appl Polym Sci. 2019;136:47663–72.
45. Kai D, Zhang K, Jiang L, Wong HZ, Li Z, Zhang Z, et al. Sustainable and antioxidant lignin–polyester copolymers and nanofibers for potential healthcare applications. ACS Sustain Chem Eng. 2017;5:6016–25.
46. Moseley R, Walker M, Waddington RJ, Chen WYJ. Comparison of the antioxidant properties of wound dressing materials–carboxymethylcellulose, hyaluronan benzyl ester and hyaluronan, towards polymorphonuclear leukocyte-derived reactive oxygen species. Biomaterials. 2003;24:1549–57.
47. Dhall S, Do DC, Garcia M, Kim J, Mirebrahim SH, Lyubovitsky J, et al. Generating and reversing chronic wounds in diabetic mice by manipulating wound redox parameters. J Diabetes Res. 2014. https://doi.org/10.1155/2014/562625.
48. Dhall S, Do D, Garcia M, Wijesinghe DS, Brandon A, Kim J, et al. A novel model of chronic wounds: importance of redox imbalance and biofilm-forming bacteria for establishment of chronicity. PLoS ONE. 2014;9:e109848.
49. Chakraborty T, Balusani D, Sabourin L, Renaud J, Sumarah M, Nakhla G, et al. Fate of micropollutants in chemically enhanced primary treatment using recovered coagulants. J Environ Manage. 2020;269: 110815.
50. Daniel G, Marie-Pierre H, Denis M. Iron-Chelating activity of tetracyclines and its impact on the susceptibility of Actinobacillus actinomycetemcomitans to these antibiotics. Antimicrob Agents Chemother. 2000;44:763–6.
51. Domínguez-Robles J, Mancinelli C, Mancuso E, García-Romero I, Gilmore BF, Casettari L, et al. 3D printing of drug-loaded thermoplastic polyurethane meshes: a potential material for soft tissue reinforcement in vaginal surgery. Pharmaceutics. 2020. https://doi.org/10.3390/pharmaceutics12010063.
52. Mathew E, Domínguez-Robles J, Stewart SASA, Mancuso E, O'Donnell K, Larrañeta E, et al. Fused deposition modeling as an effective tool for anti-infective dialysis catheter fabrication. ACS Biomat Sci Eng. 2019;5:6300–10.
53. Jo YK, Heo S-J, Peredo AP, Mauck RL, Dodge GR, Lee D. Stretch-responsive adhesive microcapsules for strain-regulated antibiotic release from fabric wound dressings. Biomater Sci. 2021;9:5136–43.
54. Domínguez-Robles J, Cárcamo-Martínez Á, Stewart SA, Donnelly RF, Larrañeta E, Borrega M. Lignin for pharmaceutical and biomedical applications—could this become a reality? Sustain Chem Pharm. 2020;18:100320.
55. Dong X, Dong M, Lu Y, Turley A, Jin T, Wu C. Antimicrobial and antioxidant activities of lignin from residue of corn stover to ethanol production. Ind Crops Prod. 2011;34:1629–34.
56. Burugapalli K, Razavi M, Zhou L, Huang Y. Cytocompatibility study of a medical <I>β</I>-type Ti-35.5Nb-5.7Ta titanium alloy. J Biomater Tissue Eng. 2016;6:141–8.
57. Avti PK, Caparelli ED, Sitharaman B. Cytotoxicity, cytocompatibility, cell-labeling efficiency, and in vitro cellular magnetic resonance imaging of gadolinium-catalyzed single-walled carbon nanotubes. J Biomed Mater Res Part A. 2013;101:3580–91.
58. Picco CJ, Domínguez-Robles J, Utomo E, Paredes AJ, Volpe-Zanutto F, Malinova D, et al. 3D-printed implantable devices with biodegradable rate-controlling membrane for sustained delivery of hydrophobic drugs. Drug Deliv. 2022;29:1038–48.
59. Lin N, Dufresne A. Nanocellulose in biomedicine: current status and future prospect. Eur Polym J. 2014;59:302–25.
60. Wang L, Zhu H, Xu G, Hou X, He H, Wang S. A biocompatible cellulose-nanofiber-based multifunctional material for Fe 3+ detection and drug delivery. J Mater Chem C. 2020;8:11796–804.
61. Figueiredo P, Lintinen K, Kiriazis A, Hynninen V, Liu Z, Bauleth-Ramos T, et al. In vitro evaluation of biodegradable lignin-based nanoparticles for drug delivery and enhanced antiproliferation effect in cancer cells. Biomaterials. 2017;121:97–108.
62. Miao Y, Tang Z, Zhang Q, Reheman A, Xiao H, Zhang M, et al. Biocompatible lignin-containing hydrogels with self-adhesion, conductivity, UV shielding, and antioxidant activity as wearable sensors. ACS Appl Polym Mater. 2022;4:1448–56.
63. Zhou Y, Han Y, Li G, Yang S, Chu F. Lignin-Based hollow nanoparticles for controlled drug delivery: grafting preparation using β-cyclodextrin/enzymatic-hydrolysis lignin. Nanomaterials. 2019;9:997.
64. Milano S, Arcoleo F, D'Agostino P, Cillari E. Intraperitoneal injection of tetracyclines protects mice from lethal endotoxemia downregulating inducible nitric oxide synthase in various organs and cytokine and nitrate secretion in blood. Antimicrob Agents Chemother. 1997;41:117–21.
65. Ahmad A, Græsbøll K, Christiansen LE, Toft N, Matthews L, Nielsen SS. Pharmacokinetic-pharmacodynamic model to evaluate intramuscular tetracycline treatment protocols to prevent antimicrobial resistance in pigs. Antimicrob Agents Chemother. 2015;59:1634–42.

Publisher's Note

Springer Nature remains neutral with regard to jurisdictional claims in published maps and institutional affiliations.

Submit your manuscript to a SpringerOpen journal and benefit from:

- ► Convenient online submission
- ► Rigorous peer review
- ► Open access: articles freely available online
- ► High visibility within the field
- ► Retaining the copyright to your article

Submit your next manuscript at ► springeropen.com